Compressive strength of ice at impact strain rates

Hyonny Kim · John N. Keune

Abstract The compressive strength of ice was measured at high strain rates of 10^3 s^{-1} order of magnitude. Since ice compressive strength is known to be strongly dependent on strain rate, properties corresponding to high strain rates are needed for engineering predictions of the behavior of ice under dynamic crushing scenarios. The split Hopkinson pressure bar (SHPB) apparatus was used to successfully measure compressive strength over a strain rate range of 400–2,600 s^{-1}. Strain rate variation was achieved by adjusting the specimen length and the velocity of the SHPB striker bar; increased velocity and reduced specimen length produced higher strain rates. Since the compressive strength was found to be nearly uniform over the measured strain rate range, an average value of 19.7 MPa is reported. However, when comparing the present results with data in the existing literature spanning several orders of magnitude in strain rate, a trend of continuously increasing strength for strain rates beyond 10^1 s^{-1} can be observed.

Introduction

In order to analyze the dynamic failure of ice, strength properties of the ice at high rates of loading, i.e., at high strain rates, must be known. Examples of when high strain rate strength data are important include simulating hail and shed ice impacts onto vehicular structures [1, 2] and predicting the passage of ice breaker ships through ice. For aircraft structures, hail impacts are of particular concern to fragile flight control surfaces (flaps, ailerons) and rotating propulsion components such as fan and propeller blades. These impacts can occur at velocities far exceeding the terminal falling velocity of hail when accounting for the aircraft's speed and a spinning component's rotational velocity.

The mechanical properties of ice material exhibit dependency on many parameters including strain rate, temperature, confinement pressure, and orientation of loading (anisotropy). While this paper is focused on the topic of strain rate, the effects of the other aforementioned parameters, as well as a general overview of the mechanical properties of ice, can be found in the thorough review works of Mellor [3], Reich et al. [4], and Petrovic [5].

The relationship between strain rate and failure strength has been investigated by many sources including Hooke et al. [6], Mellor and Cole [7], Shen et al. [8], Kuehn et al. [9], Jones [10], and Schulson [11]. Although it has been documented that compressive strength increases with strain rates up to at least 10^{-3} s^{-1}, there are several conflicting hypotheses about what happens at higher strain rates. Jones [10] indicates that strength will keep on increasing or at least remain steady. Hooke et al. [6] states that the compressive strength could, in theory, increase up to 200 MPa. Schulson [11] indicates that strength peaks at around 10^{-2} s^{-1} and then decreases due to a transition from ductile to brittle mode of failure.

H. Kim (✉)
Department of Structural Engineering, University of California, San Diego, CA, USA
e-mail: hyonny@ucsd.edu

J. N. Keune
The Boeing Company, Everett, WA, USA

In summary, the existing literature reports the compressive strength of ice to be in the range of 1.0–15 MPa for strain rates ranging between 10^{-6} and 10^1 s^{-1}, respectively. Note that impact strain rates (10^3 s^{-1}) are significantly higher than those for which existing data are available (10^1 s^{-1} by Jones [10]). Therefore it is desirable to gather data at higher strain rates through the use of the Split Hopkinson Pressure Bar (SHPB). The SHPB is a mechanical testing apparatus designed specifically to measure high strain rate dynamic mechanical properties of materials. As reported herein, the SHPB was used to measure the dynamic compressive strength of ice at strain rates in the 10^2–10^3 s^{-1} magnitude range. These data fill a gap in the current literature, since presently available strength data exists only for strain rates up to 10^1 s^{-1} using a high-speed uniaxial test machine [10].

Specimen description

An important aspect of these experiments is the production of consistent quality ice specimens. These had to be manufactured in a repeatable manner at different lengths in order to achieve variations of strain rate. Solid cylindrical specimens of 12.7 mm diameter were cast using distilled water in specially designed closed nylon molds that consisted of a hollow cylinder body with end caps, as shown in Fig. 1. One end cap is firm-fitting and remains fixed, forming a cup, while the other is allowed to stroke (tight slip fit) and incorporates a vent hole to allow for the release of air and excess water during closing of the mold. Once filled, the molds were placed in a –16 °C freezer. Volume expansion of the water during freezing is accommodated by the sliding end cap. In order to be able to remove the ice specimens from the molds without

damaging them, it was necessary to lubricate the mold interior surfaces with a light machine oil prior to filling.

Exact specimen length was difficult to control due to the expansion of ice during phase change from water, the sliding freedom of the end cap, and the water loss through the vent hole during the freezing process. Therefore, the length of each specimen was measured just prior to testing in the SHPB (using in-situ method to be described later) to obtain accurate specimen length data which are vital for subsequent data processing.

Shortly before testing, the specimens were removed from the molds and returned back into the –16 °C freezer so the temperature can normalize. At test time, the specimens were loaded into the SHPB apparatus and tested within the time window of 2–3 min after being removed from the freezer. Since testing was not conducted in a cold environment, consistent time to test was used to control the temperature of the ice specimen. A special specimen having embedded thermocouples was used to determine that this time window corresponds to the ice temperature just reaching 0 °C. Since all specimens showed some optical cloudiness of varying degree, ten specimens were dimensionally measured and weighed to find an average density of 897 kg/m^3 (14 kg/m^3 standard deviation).

Experimental apparatus

The SHPB apparatus shown in Fig. 2 consists of polished steel bars that are guided to move only axially, strain gages, and measurement electronics. The striker bar is accelerated by pressurized gas and impacts the incident bar which sends a compressive stress pulse along the incident bar, through the specimen, and on into the transmission bar. A reflected pulse is also generated and returns back through the incident bar. Strain gages mounted to the incident and transmission bars are used to measure the incident, transmitted, and reflected strain pulses as a function of time. From these strain measurements, since the steel bars have known properties, the stress and strain within the specimen can be calculated without knowing the specimen's properties a priori. Electronic equipment used for data measurement are Tektronix AM 502 amplifiers and a Tektronix TDS 420 oscilloscope.

Since the SHPB was not located within a cold environment chamber, prior to testing, the steel bars contacting the specimens must be cooled so as to reduce the rate at which the ice melts when contacting these bars. Bags of ice were placed in contact with the top and bottom of the incident and transmission bars at
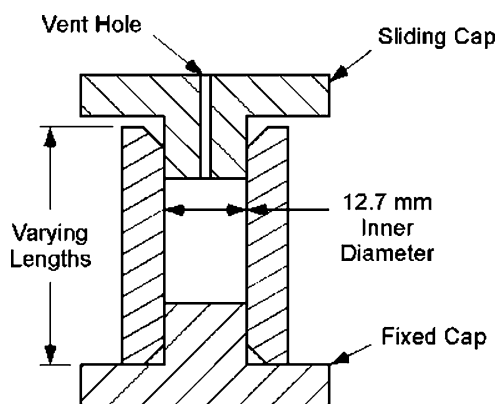
Fig. 1 Nylon mold for casting cylindrical ice specimens
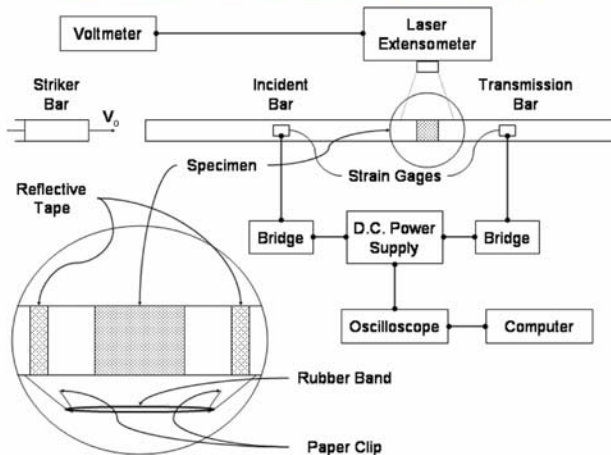
Fig. 2 Split Hopkinson Pressure Bar

the specimen test location for 1 h prior to the testing. The ice bags were removed at the time of specimen testing, and were reapplied for 30 min duration after every eight specimen tests.

Due to surface-contact melting, the specimen length is continuously changing. Thus a laser extensometer (Electronic Instrument Research Ltd. Model LE-05) was used to measure the distance between two reflective tapes located on the steel bars (see inset in Fig. 2) to provide an accurate measurement of the ice specimen length at the exact time of firing. Accurate length measurement is needed for post-processing the raw data into strain and strain rate quantities. The rubber band shown in Fig. 2 provided light clamping force of the bars onto the specimen in order to keep the specimen in place and to prevent any initial gaps (air or water filled) between the specimen and the bars.

Data measurement and processing

The compressive stress pulse is measured with strain gages located on the incident and transmission bars. At each strain gage location, two gages are affixed

opposite each other on the radial surfaces of the bars. These two gages are connected in a Wheatstone bridge so as to cancel the effects of bending wave induced readings that may exist. Three voltage signals are simultaneously measured for each test and are shown in Fig. 3. These are the incident, reflected and transmitted pulses.

The raw voltages in Fig. 3 are converted into the strains measured in the steel bars, which are then used to calculate the strain, strain-rate and stress within the specimen using one-dimensional elastic wave theory. Equations 1–3 are used to perform these calculations [12, 13].

$$\varepsilon_S = \frac{c_0}{L_0} \int_0^t (\varepsilon_I - \varepsilon_R - \varepsilon_T) dt' \tag{1}$$

$$\dot{\varepsilon}_S = \frac{c_0}{L_0} (\varepsilon_I - \varepsilon_R - \varepsilon_T) \tag{2}$$

$$\sigma_S = 1/2 E \left(\frac{A}{A_S}\right) (\varepsilon_I + \varepsilon_R + \varepsilon_T) \tag{3}$$

In Eqs. 1–3, strains are symbolized as ε with subscripts denoting incident (I), reflected (R), transmitted (T), or within specimen (S). The stress in the specimen is σ_S and specimen cross-section area is A_S. Steel bar properties in these equations are the elastic wave velocity ($c_0 = 5{,}200$ m/s), elastic modulus ($E = 210$ GPa) and area ($A = 127$ mm^2). The ice specimen initial length L_0 is the value measured at the time of testing, as previously discussed. It is important to note that in the application of these
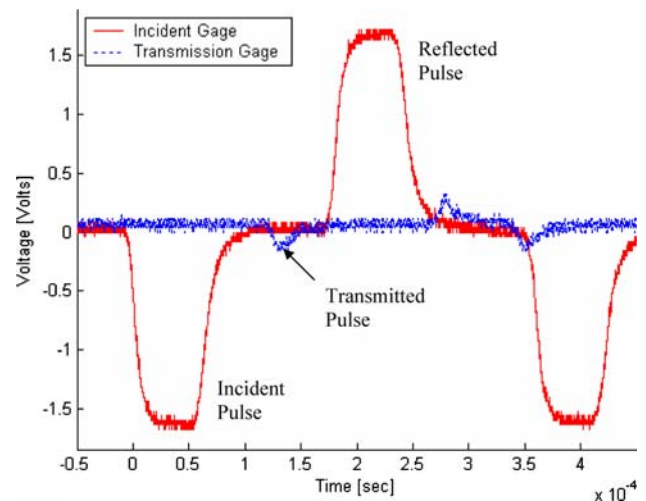

Fig. 3 Typical SHPB raw voltage data (specimen ID: ice_50_34)

equations, the strain pulses (ε_I, ε_R and ε_T) from Fig. 3 are shifted along the time axis, using the known distance between each strain gage and the specimen together with the elastic wave speed c_0, so as to be coincident at the specimen.
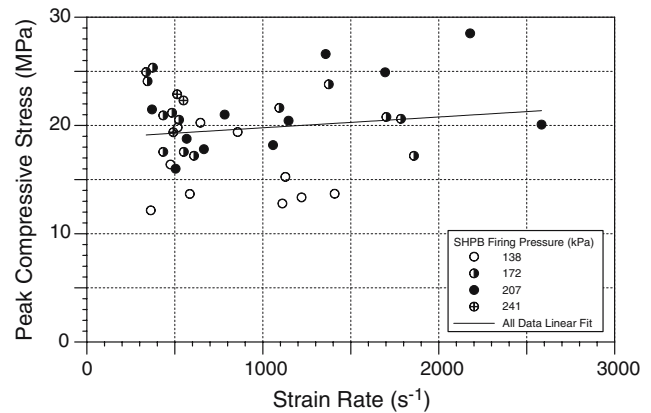
Results

Successful measurements were obtained from 38 tests, with those in which errors occurred in the data collection not being reported. Varying combinations of specimen length and striker bar firing pressure were used to achieve strain rates ranging from 400 to 2,600 s^{-1}. Figure 4 reports the measured strain rate at the time of peak stress as a function of specimen length for varying incident bar firing pressures. As expected, the smaller specimen length produces higher strain rates. Fits to the 138 kPa and 207 kPa data are shown in the plot. These fitting functions are of the general form α/L_o where α is is an arbitrary fitting constant. The 138 kPa fit matches the data with an R^2 value of 0.898, and the 207 kPa fit matches the data with an R^2 value of 0.910, thereby confirming that the relationship between strain rate and specimen length L_o follows Eq. 2.

Figure 5 reports the measured peak stress as a function of strain rate corresponding to the time of peak stress for different SHPB firing pressures. Since these data show little dependency of strength on strain rate across this range, the data were pooled as one set having an average compressive strength of 19.7 MPa (3.9 MPa standard deviation). Thus 19.7 MPa compressive strength can be associated with 10^3 s^{-1} magnitude strain rate.
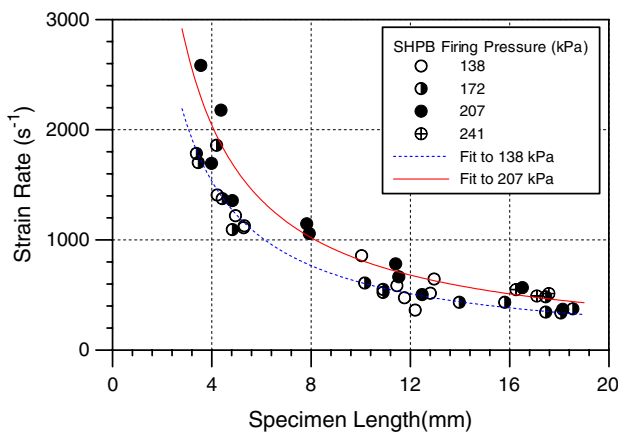
**Fig. 4** Strain rate variation with specimen length

Fig. 5 High strain rate compressive strength measured by SHPB

Discussion

Figure 6 plots the present results together with data reported by Mellor and Cole [7], Shen et al. [8], Kuehn et al. [9], and Jones [10]. As previously mentioned, researchers have expressed conflicting hypotheses regarding the dependency of compressive strength on strain rate well beyond the range of 10^{-2}–10^{-3} s^{-1}. This range has been observed to be a transition point of ductile-to-brittle ice mechanical behavior by Schulson [11, 14]. The highest strain rate at which existing compressive strength data have been previously reported is at 10^1 s^{-1} by Jones [10]. When comparing Jones [10] data with the other researchers' data, as summarized in Fig. 6, a trend can be observed of increasing strength at strain rates higher than the plateau-like trend between 10^{-3} and 10^0 s^{-1}. The presently reported data are consistent with the rising trend established by Jones [10] and indicate a significant increase of compressive strength for strain rates having 10^3 s^{-1} order of magnitude.

Like the data of other researchers, the present results show significant scatter. These are attributed to several factors. Foremost of these is specimen quality, as indicated by the variation in specimen density. Additionally, some internal whitening was occasionally observed upon removing a specimen from the mold. These specimens were tested unless external cracking was visible. The effects of localized melting at the specimen-to-bar contact locations is unknown. It is hypothesized that a thin layer of water accumulating between the ice specimen and bars could affect the results, primarily via increased elastic wave reflection due to higher acoustic impedance at the bi-material interfaces (e.g., liquid water/

Fig. 6 Comparison of SHPB data with strength reported in existing literature
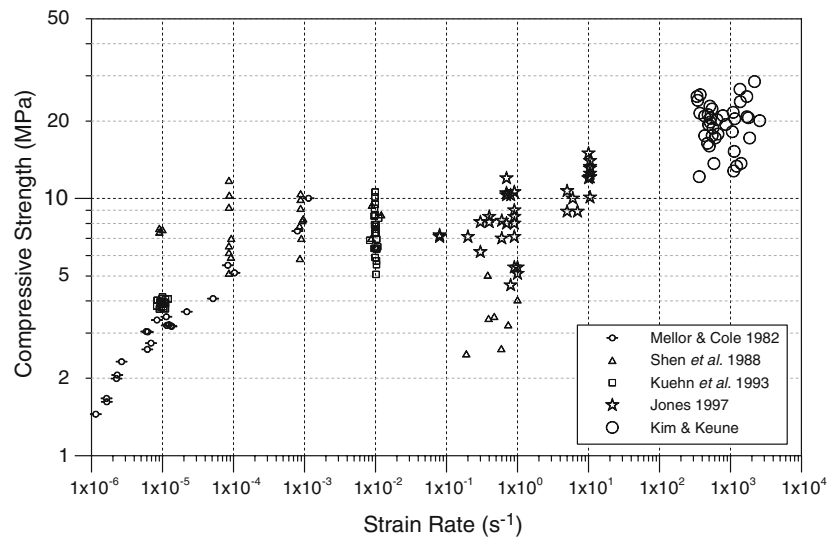
steel and water/ice). Conducting tests in a cold temperature controlled environment would eliminate the melting issue, potentially reducing scatter.

All tests correspond to an ice specimen temperature of 0 °C. Since the compressive strength of ice is known to increase with decreasing temperature [14], the data presented herein can be considered as low-bounding values of compressive strength in the range of 10^3 s^{-1} strain rate.

Conclusions

The Split Hopkinson Pressure Bar (SHPB) was used to measure the dynamic compressive strength of ice at strain rates between 400 and 2,600 s^{-1}. The average strength over this range of strain rates is 19.7 MPa (3.9 MPa standard deviation). While strength measurements were found to be nearly uniform over this range, comparison of these data with those previously reported in the existing literature shows a trend of continually increasing compressive strength for strain rates beyond 10^1 s^{-1} (previous highest strain rate for which strength data were reported). The SHPB was found to be a capable test instrument for measuring ice strength at impact strain rates. Consistent strain rate was found to be repeatable and controllable by adjusting specimen length, and is shown to closely follow a $1/L_0$ relationship.

References

1. Kim H, Kedward KT (2000) AIAA J 38(7):1278
2. Kim H, Kedward KT, Welch DA (2003) Compos Part A 34(1):25
3. Mellor M (1979) In: Tryde P (ed) Physics and mechanics of ice. IUTAM Symposium, Copenhagen, pp 217–245
4. Reich AD, Scavuzzo RJ, Chu ML (1994) Survey of mechanical properties of impact ice. Proceedings of 32nd aerospace sciences meeting and exhibit, AIAA 94–(0712) January 10–13, Reno, NV
5. Petrovic JJ (2003) Review mechanical properties of ice and snow. J Mater Sci 38:1
6. Hooke R LeB, Mellor M, Budd WF, Glen JW, Higashi A, Jacka TH, Jones SJ, Lile RC, Martin RT, Meier MF, Russel-Head DS, Weeterman J. (1980) Cold Regions Sci Technol 3:263
7. Mellor M, Cole DM. (1982) Cold Regions Sci Technol 5(3):201
8. Shen, L-T, Zhao, S-D, Lu, X-N, Shi, Y-X (1988) In: Proceedings of the seventh international conference on offshore mechanics and arctic engineering, American Society of Mechanical Engineers, New York, pp 19–23
9. Kuehn GA, Schulson EM, Jones D E, Zhang J. (1993) J Offshore Mech Arctic Eng, Trans ASME 115(2):142
10. Jones SJ. (1997) J Phys Chem B 101(32):6099
11. Schulson EM. (1997) J Phys Chem B 101(32):6254
12. Lindholm US. (1964) J Mech Phys Solids 12:317
13. Follansbee PS, Frantz C. (1983) J Eng Mater Technol 105:61
14. Schulson EM, (1990) Acta Metall Mater 38(10):1963